Theoretical study of the phonon spectra of multiferroic $BiFeO_3$ nanoparticles

2009 J. Phys.: Condens. Matter 21 036002

(http://iopscience.iop.org/0953-8984/21/3/036002)

J. Phys.: Condens. Matter **21** (2009) 036002 (9pp) doi:10.1088/0953-8984/21/3/036002

Theoretical study of the phonon spectra of multiferroic $BiFeO_3$ nanoparticles

I Apostolova[1], A T Apostolov[2] and J M Wesselinowa[3]

[1] Faculty of Forest Industry, University of Forestry, Boulevard Kliment Okhridsky 10, 1756 Sofia, Bulgaria
[2] Department of Applied Physics, Technical University, Boulevard Kliment Okhridsky 8, 1000 Sofia, Bulgaria
[3] Department of Physics, University of Sofia, Boulevard J. Bouchier 5, 1164 Sofia, Bulgaria

Received 27 September 2008, in final form 14 November 2008
Published 17 December 2008
Online at stacks.iop.org/JPhysCM/21/036002

Abstract
The phonon properties of multiferroic $BiFeO_3$ (BFO) nanoparticles are studied using a Green's function technique on the basis of the Heisenberg and the transverse Ising models, taking into account anharmonic spin–phonon and phonon–phonon interaction terms. The phonon spectrum is obtained for different exchange, magnetoelectric, and spin–phonon interaction constants. The influence of temperature, surface and size effects on the phonon energy and damping is discussed. The phonon energy and damping in BFO nanoparticles are greater in comparison to those in bulk BFO. The strong spin–phonon interactions lead to anomalies in the phonon spectrum around the magnetic and ferroelectric phase transitions. The influence of an applied magnetic field is studied, too. The predictions are consistent with experimental results.

1. Introduction

Magnetoelectric multiferroics, materials which exhibit simultaneous magnetic and ferroelectric order, have attracted a lot of attention in the last few years because of their potential for cross electric and magnetic functionality [1]. A fundamental understanding and experimental observation of the coupling mechanism between the (anti)ferroelectric and (anti)ferromagnetic order are of great interest. However, very little is known about the behavior of phonons in magnetoelectric multiferroics, especially in multiferroic nanostructures, although investigations of phonons have in the past played a crucial role in the understanding of classic ferroelectrics (FEs). Phonons are also known to be influenced by spin correlation thus offering a complementary tool [2]. Recent investigations by Raman and infrared spectroscopy, by transmittance and reflectance measurements have revealed the importance of phonon effects in multiferroics. There is experimental evidence for a strong spin–phonon coupling in these substances [3–5]. One of the natural ferroelectromagnets is $BiFeO_3$ (BFO), which exhibits both ferroelectricity and ferromagnetism (i.e. multiferroism, $T_C = 1100$ K, $T_N = 643$ K), an intrinsic multifunctionality that would ostensibly make it a strong candidate for nanoscale electronics applications. In order to determine and understand the role of phonons in multiferroics, Haumont *et al* [6] have undertaken a first-time Raman scattering study of BFO. Their experimental results reveal pronounced phonon anomalies around the magnetic phase transition temperature. These anomalies are attributed to the multiferroic character of the materials. Fukumura *et al* [7] have reported detailed Raman spectra of BFO single crystals in the temperature range 4–1100 K, and consider coupling of phonons with the magnetic ordering and the structural phase transition. Singh *et al* [8] have observed Raman scattering from magnons in the frequency range from 10 to 65 cm^{-1} in BFO single crystals at cryogenic temperatures. Raman spectra of BFO multiferroic ceramics have been reported by Yuan *et al* [9], Kamba *et al* [10] and Seidel *et al* [11]. Lobo *et al* [12] discussed the infrared reflectivity measurement on a multiferroic BFO single crystal between 5 K and room temperature. Their findings show that the softening of the lowest frequency E mode is responsible for the temperature dependence of the dielectric constant, indicating that the ferroelectric transition in BFO is soft-mode driven. Recently, Singh *et al* [13, 14] first observed room-temperature spectra with phonon mode assignments of the $(111)_c$-oriented BFO epitaxial films with rhombohedral $R3c$ symmetry and the $(001)_c$-oriented BFO epitaxial films with pseudo-tetragonal symmetry. The phonon frequencies in BFO thin films [13] are greater in comparison to those in bulk BFO [6]. Bea *et al* [15] have studied the Raman spectra of BFO thin films and observed also that both the unpolarized and polarized Raman

spectra are different from those of bulk BFO [6]. Using the polymerized complex method, Popa *et al* [16] have prepared single-phase BFO powders with particle size from 7 to 11 nm, which have been investigated by Raman spectroscopy between 350 and 600 °C. The obtained reduced intensities and widened bands could be related to the average crystal size within the powder particles.

In order to explain the experimentally observed enhanced polarization and magnetization in multiferroic nanoparticles, we have investigated in our previous paper [17] the influence of the surface and the particle size on ferromagnetic and ferroelectric properties based on two microscopic models—the modified Heisenberg and the transverse Ising model and material specific coupling term. The coupling between electric and magnetic polarizations in multiferroic BFO nanoparticles is demonstrated by studying the effect of an external magnetic field on different ferroelectric properties [18]. The aim of the present paper is to extend our previous one [17] and to apply the microscopic model including the spin–phonon interactions to study the optical phonon spectra in BFO nanoparticles.

2. The model

The Hamiltonian of the multiferroic system which is appropriate for hexagonal $RMnO_3$ and BFO can be presented as:

$$H = H^{\mathrm{m}} + H^{\mathrm{e}} + H^{\mathrm{me}}. \tag{1}$$

H^{m} is the Hamiltonian for the magnetic subsystem, which is given by the Heisenberg Hamiltonian:

$$H^{\mathrm{m}} = -\tfrac{1}{2}\sum_{\langle ij\rangle} A_1(i,j)\mathbf{B}_i\cdot\mathbf{B}_j - \tfrac{1}{2}\sum_{[ij]} A_2(i,j)\mathbf{B}_i\cdot\mathbf{B}_j - g\mu_{\mathrm{B}}H\sum_i B_i^z, \tag{2}$$

where B_i is the Heisenberg spin at the site i, and the exchange integrals $A_1 > 0$ and $A_2 < 0$ represent the coupling between the nearest and next-nearest neighbors, respectively. H is the external magnetic field parallel to the z axis. $\langle ij\rangle$ and $[ij]$ denote the single summation over the nearest neighbors and the next-nearest neighbors, respectively. We take $A_1 = A_{1s}$, $A_2 = A_{2s}$ on the surface of the particle and A_1, A_2 in the particle. The notation s is used to describe all interaction constants on the surface.

H^{e} denotes the Hamiltonian for the electrical subsystem which is dealt within the framework of the transverse Ising model (TIM). Thus H^{e} in the presence of an electric field can be written as:

$$H^{\mathrm{e}} = -\Omega\sum_i S_i^x - \tfrac{1}{2}\sum_{ij} J_{ij}S_i^zS_j^z - \mu E\sum_i S_i^z, \tag{3}$$

where S_i^x, S_i^z are the spin-1/2 operators of the pseudo-spins, E represents the external electric field, $J_{ij} > 0$ denotes the nearest-neighbor pseudo-spin interaction, and Ω is the tunneling frequency. Blinc and de Gennes proposed the TIM for the description of order–disorder KDP-type FEs [19]. For H-bonded FEs the transverse field represents the proton tunneling between the two equilibrium positions on the H-bonds. Further, the TIM is applied to displacive type FEs such as $BaTiO_3$ (BTO) [20, 21], too. According to the order–disorder model, the disorder in the paraelectric phase in BTO is associated with the position of the Ti ions. Instead of occupying the body center positions as in an ideal cubic perovskite structure, the Ti ions are randomly displaced along the cube diagonals causing disorder. In the case of a tunneling frequency very small with respect to the interaction constant, one may use the TIM as a model for order–disorder FEs without tunneling motion (e.g. for $NaNO_2$, TGS). Therefore the TIM can be applied to describe the electric polarization in all types of FEs. The mean electric polarization is proportional to the z component of the pseudo-spins introduced in the TIM. In the ordered phase we have the mean values $\langle S^x\rangle \neq 0$ and $\langle S^z\rangle \neq 0$, and it is appropriate to choose a new coordinate system rotating the original one used in (2) by the angle θ in the xz plane. The rotation angle θ is determined by the requirement $\langle S^{x'}\rangle = 0$ in the new coordinate system.

The most important term is H^{me} which describes the coupling between the magnetic and the electric subsystems in the ferroic compound, and can be applied to hexagonal multiferroic $RMnO_3$ compounds and to $BiFeO_3$:

$$H^{\mathrm{me}} = -g\sum_{\langle ij\rangle}\sum_{kl} S_k^zS_l^z\mathbf{B}_i\cdot\mathbf{B}_j. \tag{4}$$

Here g is the coupling constant between the magnetic and the electric order parameters. It must be noted here that the orthorhombic perovskite $RMnO_3$ and the hexagonal $RMnO_3$ are in very different classes of magnetoelectrics. The use of the TIM and biquadratic coupling between the pseudo-spins and magnetic moments implies that the magnetic and ferroelectric orderings have independent mechanisms. In particular, this generally leads to different transition temperatures for the two subsystems. The model with biquadratic coupling between the pseudo-spins and the magnetic moments can be applied to multiferroic substances where $T_{\mathrm{C}} \gg T_{\mathrm{N}}$, for example in hexagonal $RMnO_3$ and $BiFeO_3$ [22]. In the orthorhombic perovskite $RMnO_3$ [23] the leading magnetoelectric interaction term is linear in the electrical dipole moment, due to the improper nature of its ferroelectricity. The same applies to RMn_2O_5, which is also an improper ferroelectric.

In order to investigate the phonon spectrum and the experimentally obtained strong spin–phonon coupling we have to include the following two terms in the Hamiltonian in equation (1):

$$H' = H_{\mathrm{ph}} + H_{\mathrm{sp-ph}}. \tag{5}$$

The first term H_{ph} contains the lattice vibrations including anharmonic phonon–phonon interactions:

$$H_{\mathrm{ph}} = \frac{1}{2!}\sum_i(\omega_i^0)^2a_ia_i^+ + \frac{1}{3!}\sum_{i,j,r}B^{\mathrm{ph}}(i,j,r)Q_iQ_jQ_r + \frac{1}{4!}\sum_{i,j,r,s}A^{\mathrm{ph}}(i,j,r,s)Q_iQ_jQ_rQ_s, \tag{6}$$

where Q_i and ω_i^0 are the normal coordinate and frequency, respectively, of the lattice mode. The vibrational normal coordinate Q_i can be expressed in terms of phonon creation and annihilation operators: $Q_i = (2\omega_i^0)^{-1/2}(a_i + a_i^+)$.

$H_{\rm sp}$ describes the interaction of the spins with the phonons:

$$H_{\rm sp} = -\tfrac{1}{2}\sum_{i,j,k}\bar{F}_{\rm m}(i,j,k)Q_i B_j^z B_k^z - \tfrac{1}{4}\sum_{i,j,r,s}\bar{R}_{\rm m}(i,j,r,s)Q_i Q_j B_r^z B_s^z + {\rm h.c.} - \tfrac{1}{2}\sum_{i,j}\bar{F}_{\rm e}(i,j)Q_i S_j^z - \tfrac{1}{4}\sum_{i,j,r}\bar{R}_{\rm e}(i,j,r)Q_i Q_j S_r^z + {\rm h.c.}, \quad (7)$$

where the indices 'e' and 'm' in the interaction constants denote the interaction of the phonons with the pseudo-spins and the magnetic spins, respectively. The first and third terms in equation (7) describe spin–phonon interaction effects arising from the first powers, whereas the second and fourth terms denote the second powers in the relative displacement of the lattice site away from equilibrium. $F(i) = \bar{F}(i)/(2\omega_i^0)^{1/2}$ and $R(i,j) = \bar{R}(i,j)/(2\omega_i^0)^{1/2}(2\omega_j^0)^{1/2}$ designate the amplitudes for coupling phonons to the spin excitations in first and second order, respectively.

3. The phonon Green's function

In this section we present calculations for obtaining the phonon Green's function for a ferroic nanoparticle. This method seems still probably the most appropriate tool to study complex systems with low symmetry. Different to extended materials the Green's function for small particles has to be formulated in real space. A magnetic nanoparticle is defined by fixing the origin of a certain spin in the center of the particle and including all spins within the particle into shells. The shells are numbered by $n = 0, \ldots, N$, where $n = 0$ denotes the central spin and $n = N$ represents the surface shell of the system.

Macroscopic and microscopic quantities can be calculated by using the retarded Green's function which is defined as:

$$G_{rs}(t) = -{\rm i}\theta(t)\langle[a_r(t); a_s^+]\rangle. \quad (8)$$

The phonon energies ω_{rs} and their damping γ_{rs} are calculated using the method of Tserkovnikov [24]. After a formal integration of the equation of motion for the Green's function (8), one obtains

$$G_{rs}(t) = -{\rm i}\theta(t)\langle[a_r; a_s^+]\rangle \exp(-{\rm i}\omega_{rs}(t)t) \quad (9)$$

where

$$\omega_{rs}(t) = \omega_{rs} - \frac{\rm i}{t}\int_0^t {\rm d}t' t' \left(\frac{\langle[j_r(t); j_s^+(t')]\rangle}{\langle[a_r(t); a_s^+(t')]\rangle} - \frac{\langle[j_r(t); a_s^+(t')]\rangle\langle[a_r(t); j_s^+(t')]\rangle}{\langle[a_r(t); a_s^+(t')]\rangle^2}\right) \quad (10)$$

with the notation $j_r(t) = \langle[a_r, H_{\rm int}]\rangle$. The time-independent term

$$\omega_{rs} = \frac{\langle[[a_r, H]; a_s^+]\rangle}{\langle[a_r; a_s^+]\rangle} \quad (11)$$

is the phonon energy in the generalized Hartree–Fock approximation (GHFA). The time-dependent term in equation (10) includes damping effects.

For the phonon energies after neglecting the transverse spin correlation functions $\langle B_i^+ B_j^-\rangle$ and decoupling of the longitudinal correlation functions $\langle B_i^z B_j^z\rangle \rightarrow \langle B_i^z\rangle\langle B_j^z\rangle$ we obtain the following expression in the size-dependent GHFA:

$$\omega_{rs}^2 = (\omega_r^0)^2 - 2\omega_r^0\delta_{rs}\left(\tfrac{1}{2}\langle S_r^z\rangle\cos\theta R_{r,e} + \frac{1}{2N^2}\sum_{ij}R_{ijrs,m}\langle B_i^z\rangle\langle B_j^z\rangle - \frac{1}{N}\sum_i B_{irs}^{\rm ph}\langle Q_i\rangle - \frac{1}{2N^2}\sum_{ij}A_{ijrs}^{\rm ph}(1+2\langle a_i^+ a_j\rangle)\right) \quad (12)$$

with

$$\langle Q_r\rangle = \left\{\langle S_r^z\rangle\cos\theta F_{r,e} + \frac{1}{2N^2}\sum_{ij}F_{ijr,m}\langle B_i^z\rangle\langle B_j^z\rangle - \frac{1}{N^2}\sum_{ij}B_{ijr}^{\rm ph}(1+2\langle a_i^+ a_j\rangle)\right\}\left\{\omega_r^0 - \langle S_r^z\rangle\cos\theta R_{r,e} - \frac{1}{2N^2}\sum_{ij}R_{ijr,m}\langle B_i^z\rangle\langle B_j^z\rangle + \frac{1}{2N^2}\sum_{ij}A_{ijr}^{\rm ph}(1+2\langle a_i^+ a_j\rangle)\right\}^{-1}. \quad (13)$$

$M = \langle B_i^z\rangle$ is the local magnetization and $P = \langle S_i^z\rangle$ is the local polarization of the nanoparticle, which are calculated from the spin Green's functions [17]. The phonon frequency ω is at first renormalized owing to the anharmonic phonon–phonon and spin–phonon interactions. If they are not taken into account, then ω is identical to the energy ω^0 of the uncoupled optical phonon. It will be independent of temperature. The calculations demonstrate that, if we want to obtain a correct temperature dependence of the phonon modes in ferroic nanoparticles, we must not neglect the effects of spin ordering, and the Hamiltonian which describes the system must include terms taking into account not only the anharmonic phonon–phonon interaction but also the anharmonic spin–phonon interaction. Moreover, the phonon frequency is renormalized also through the magnetoelectric coupling g which is included in the calculation of the magnetization M.

The experimentally obtained broadened peaks in the Raman spectra of nanoparticles, and especially of BFO ceramics [11] and nanoparticles [16] cannot be understood within the random phase approximation (RPA) for small particles. We go beyond the RPA and calculate the phonon damping effects in multiferroic nanoparticles, taking into account anharmonic phonon–phonon and spin–phonon interactions. Then we obtain the following expression for the phonon damping:

$$\gamma(rs) = \gamma_{\rm ph-ph}(rs) + \gamma_{\rm sp-ph}(rs). \quad (14)$$

$\gamma_{\rm ph-ph}$ is the damping part which arises from the phonon–phonon interaction:

$$\gamma_{\rm ph-ph}(rs) = \frac{3\pi}{N^2}\sum_{ij}(B_{ijr}^{\rm ph})^2(\bar{n}_i - \bar{n}_j) \times \delta_{rs}[\delta(-\omega_i - \omega_j + \omega_r) - \delta(\omega_i - \omega_j + \omega_r)]$$

$$+\frac{4\pi}{N^3}\sum_{ijl}(A^{\rm ph}_{ijlr})^2\delta_{rs}[\bar{n}_i(1+\bar{n}_j+\bar{n}_l)-\bar{n}_j\bar{n}_l]$$
$$\times\delta(\omega_i-\omega_j+\omega_l-\omega_r). \quad (15)$$

$\gamma_{\rm sp-ph}(rs)$ is the damping due to the spin–phonon interactions:

$$\gamma_{\rm sp-ph}(rs)=\frac{\pi}{4}\langle S^z_r\rangle\sin^2\theta F^2_{rs,e}\delta_{rs}\delta(E_r-\omega_s)$$
$$+\frac{\pi}{4N^2}\sin^2\theta\sum_{ij}R^2_{ijr,e}\langle S^z_r\rangle(\bar{n}_i-\bar{L}_j)\delta_{rs}\delta(\omega_i-E_j-\omega_r)$$
$$+\frac{\pi}{N^3}\cos^2\theta\sum_{ijl}R^2_{ijlr,e}\langle S^z_r\rangle\delta_{rs}[\bar{L}_i(1+\bar{n}_j+\bar{L}_l)-\bar{n}_j\bar{L}_l]$$
$$\times\delta(E_i-E_j-\omega_l+\omega_r)$$
$$+\frac{2\pi}{N^2}\sum_{ij}F^2_{ijr,m}\langle B^z_i\rangle\langle B^z_j\rangle(\bar{N}_i-\bar{N}_j)\delta_{rs}\delta(\epsilon_i-\epsilon_j-\omega_r)$$
$$+\frac{2\pi}{N^3}\sum_{ijl}R^2_{ijlr,m}\langle B^z_i\rangle\langle S^z_j\rangle\delta_{rs}[(\bar{N}_i-\bar{N}_j)(1+\bar{n}_l)$$
$$+\bar{N}_i(1+\bar{N}_j)+\langle S^z_i\rangle\langle S^z_j\rangle]\delta(\epsilon_i-\epsilon_j-\omega_l+\omega_r). \quad (16)$$

E_i and ϵ_i are the excitations in the electric and magnetic systems, respectively, observed in [17]. $\bar{N}_i=\langle B^-_i B^+_i\rangle$, $\bar{L}_i=\langle S^-_i S^+_i\rangle$, and $\bar{n}_i=\langle a^+_i a^-_i\rangle$ are correlation functions which are calculated via the spectral theorem. For low temperatures, the spin–phonon and phonon–phonon interactions contribute to the damping, whereas in the vicinity of and above $T_{\rm C}$ only the anharmonic phonon–phonon interaction terms from equation (15) remain.

4. Numerical results and discussion

In [2] we have calculated the temperature dependence of the phonon energy of hexagonal bulk multiferroics for different anharmonic spin–phonon interactions $R_{\rm e}$ and $R_{\rm m}$ constants which can be positive, $R>0$, or negative, $R<0$. The frequency shift below $T_{\rm N}$ and $T_{\rm C}$ can be explained only if we assume a spin-dependent force constant given by the first and second derivatives of the magnetic exchange interaction $A_1(r_i-r_j)$ (or J_{ij} for the ferroelectric system) between the ith and jth ions with respect to the phonon displacements u_i, u_j. This displacement is interpreted by taking the nearest-neighbor exchange integral $A_1(r_i-r_j)$ (or J_{ij}) and the next-nearest-neighbor magnetic exchange integral $A_2(r_i-r_j)$ (or K_{ij} for the ferroelectric system). The squared derivatives of A_1 and A_2 (or J and K) with respect to the phonon displacement can have opposite signs. But the competition between the exchange interaction of nearest and next-nearest neighbors is only one of the possible explanations. In principle, the different sign of R can be connected also with different strains due to the influence of defects and mechanical strain, with different ordering in the shells and between the shells in nanoparticles etc.

In this section we shall present the numerical calculations of our theoretical results for multiferroic nanoparticles, taking the following model parameters which are appropriate for $BiFeO_3$ with $T_{\rm N}=640$ K and $T_{\rm C}=1100$ K: $A_1=35$ K, $A_2=-20$ K, $\Omega=20$ K, $J=2350$ K, $g=50$ K, $\omega_0=340$ cm^{-1}, $F_{\rm e}=F_{\rm m}=10$ cm^{-1}, $R_{\rm m}=-6$ cm^{-1}, $R_{\rm e}=-50$ cm^{-1}, $A^{\rm ph}=-5$ cm^{-1}, $B^{\rm ph}=0.5$ cm^{-1},

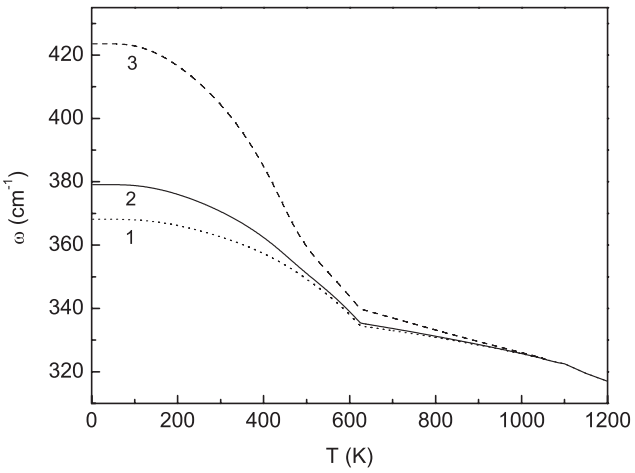

Figure 1. Temperature dependence of the phonon energy ω for a multiferroic nanoparticle with $N=4$ shells and different surface interaction constants: (1) $R_{\rm ms}/R_{\rm m}=0.2$, $R_{\rm es}/R_{\rm e}=0.2$; (2) $R_{\rm ms}/R_{\rm m}=1$, $R_{\rm es}/R_{\rm e}=1$; (3) $R_{\rm ms}/R_{\rm m}=5$, $R_{\rm es}/R_{\rm e}=5$.

$S=2.5$ for the magnetic spins and $S=0.5$ for the pseudo-spins. The crystalline lattice spacing in nanoparticles, for example, can be altered by surface relaxation, stress, or strain. It is now established that for the case of real crystals, when their dimensions are relatively small, surface modes and effects of the dimensions will also manifest themselves in addition to the normal modes of the infinite lattice. We include the surface effects by different coupling parameters within the surface shell $R_{\rm ms}$ ($R_{\rm es}$), and within the bulk and between the surface and the bulk $R_{\rm m}$ ($R_{\rm e}$). Due to the changed number of next-nearest neighbors on the surface, the reduced symmetry and the changed lattice constants, the interaction constants can take different values for the surface compared to the value in the particle. We present in figure 1 the surface effects on the temperature dependence of the phonon energy ω of a multiferroic nanoparticle with $N=4$ shells for $R_{\rm m}<0$, $R_{\rm e}<0$ and different surface values $R_{\rm ms}$ and $R_{\rm es}$. We have chosen negative spin–phonon and pseudo-spin–phonon interaction constants, because they lead to the correct temperature behavior, softening of the phonon modes, obtained in BFO nanoparticles. It can be seen that for $R_{\rm ms}<R_{\rm m}$ and $R_{\rm es}<R_{\rm e}$ (curve 1) the phonon energy of the nanoparticle is smaller than the bulk one (curve 2), whereas for $R_{\rm ms}>R_{\rm m}$ and $R_{\rm es}>R_{\rm e}$ (curve 3) it is larger than for the bulk. The influence of the surface spin–phonon interaction $R_{\rm ms}$ is greater than that of the surface pseudo-spin–phonon interaction $R_{\rm es}$ (figures 2 and 3). For the case that the surface interaction constant is larger than the bulk one (curve 3), the changes in the phonon energy of the nanoparticles are stronger. With increasing of the surface anharmonic spin–phonon and pseudo-spin–phonon constants $R_{\rm ms}$ and $R_{\rm es}$, the phonon energy ω (figures 1–3) and the phonon damping γ increase (figure 4). The influence of the spin–phonon interaction constant $R_{\rm m}$ is only below $T_{\rm N}$ in the phase where ferroelectric and magnetic properties exist together, whereas $R_{\rm e}$ influences the properties in the whole temperature region $T<T_{\rm C}$. Above $T_{\rm C}$ only the anharmonic phonon–phonon interactions remain. In our

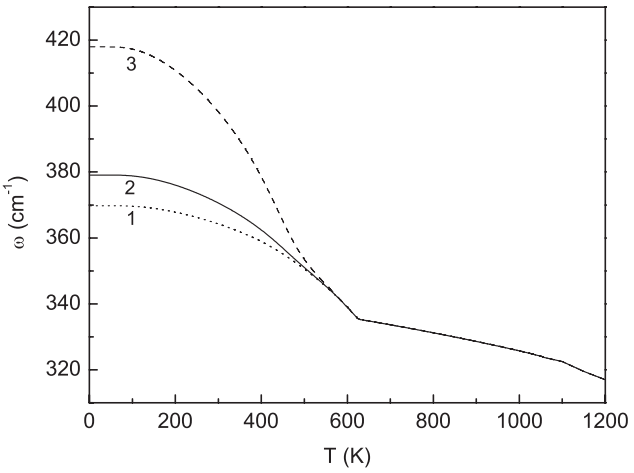

Figure 2. Temperature dependence of the phonon energy ω for a multiferroic nanoparticle with $N = 4$ shells, $R_{es}/R_e = 1$, and different surface spin–phonon interaction constants R_{ms}/R_m: (1) 0.2; (2) 1; (3) 5.

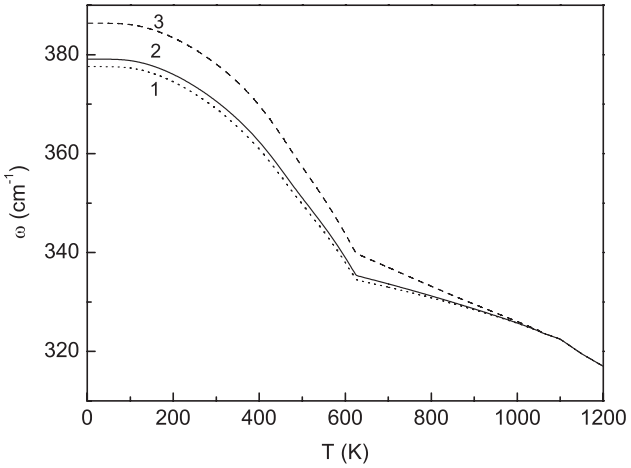

Figure 3. Temperature dependence of the phonon energy ω for a multiferroic nanoparticle with $N = 4$ shells, $R_{ms}/R_m = 1$, and different surface pseudo-spin–phonon interaction constants R_{es}/R_e: (1) 0.2; (2) 1; (3) 5.

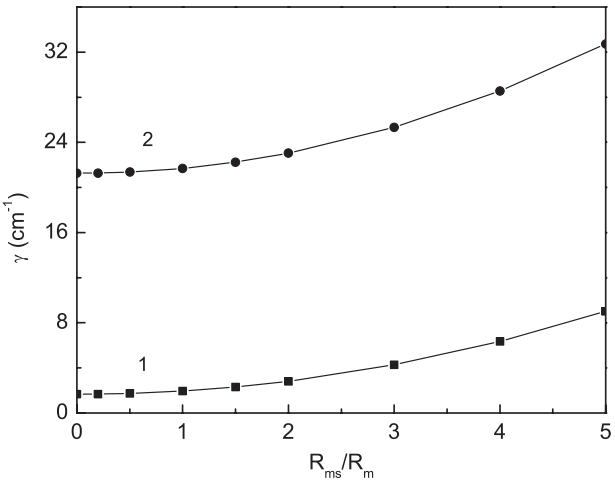

Figure 4. Dependence of the phonon damping γ on the surface spin–phonon interaction constant R_{ms} for a multiferroic nanoparticle with $N = 4$ shells, $R_{es}/R_e = 1$ and different temperatures T: (1) 100; (2) 300 K.

previous paper [25] we have shown the importance of the spin–phonon interaction R_m in ferromagnetic nanoparticles, which here also plays an important role. The temperature dependence of $\omega(T)$ including only anharmonic phonon–phonon interaction, i.e. $R_m = 0$, is very small. We have concluded that if we want to explain the experimental data of the temperature dependence of the phonon modes in magnetic nanoparticles we must take into account higher-order spin–phonon interactions, which play an important role below T_N. The nonlinear phonon spectra are due to effects of the spin ordering on the phonon properties.

The temperature dependence of the phonon mode is shown in figure 1. It can be seen that the phonon energy decreases with increasing temperature. This is in agreement with the experimental data. Lobo *et al* [12] have obtained from infrared reflectivity measurements that the E(1) mode softens strongly from 5 K to room temperature. High temperature infrared [10] and Raman [6] measurements indicate that this mode continues to soften. We obtain an anomaly, a kink around the magnetic phase transition temperature $T_N = 80$ K, but no strong phonon softening is observed near T_C. The anomaly near T_N arises from spin–phonon interactions. The phonons show a magnetic shift below T_N, where the moments of Fe start to order. The kink is due to the magnetoelectric effect, too. Above $T_C = 900$ K the phonon energy slightly decreases. The pseudo-spin–phonon interaction R_e influences mainly the phonon energy between T_N and T_C. With increasing $|R_e|$ the curve becomes steeper. The obtained temperature behavior in figure 1 with drastic changes at the two critical temperatures T_N and T_C due to a phonon coupling with the magnetic ordering and the structural phase transition, respectively, was measured in the phonon spectra of $BiFeO_3$ by Haumont *et al* [6] and Fukumura *et al* [7]. A similar phonon anomaly was observed near the Néel temperature T_N in BFO thin films by Ramirez *et al* [26], in Mn-doped BFO nanoparticles by Fukumura *et al* [27] and in $YbMnO_3$ thin films by Fukumura *et al* [28]. This was interpreted by a coupling between the phonon and magnetic spin system. Haumont *et al* [6] argued that because the frequency of the lowest mode did not vanish smoothly at the Curie temperature, the ferroelectric transition in BFO would not be soft-mode driven. This picture was later revised to propose that the incomplete phonon softening could rather be a sign of a first-order phase transition [10, 26]. However, both scenarios remained speculative. Recently, Lobo *et al* [12] have shown that the softening of the lowest frequency E(1) mode is responsible for the temperature dependence of the dielectric constant, indicating that the ferroelectric transition in BFO single crystals is soft-mode driven, contrary to the work of Hermet *et al* [29], and in agreement with Kamba *et al* [10].

The shift of the phonon spectra is dependent not only on the sign of the spin–phonon interaction constant R_m but also on the magnitude of $|R_m|$ (figures 5 and 6). With increase of the magnetic spin–phonon coupling $|R_m|$, the phonon frequency increases nearly linearly (figure 6). The

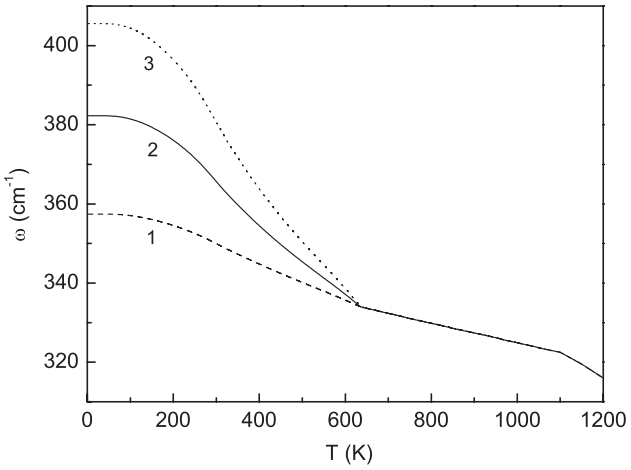

Figure 5. Temperature dependence of the phonon energy ω for a multiferroic nanoparticle with $N = 7$ shells, $R_{ms}/R_m = 1.5$, $R_{es}/R_e = 1.5$, and different bulk spin–phonon interaction constants $|R_m|$: (1) 2; (2) 6; (3) 10 cm^{-1}.

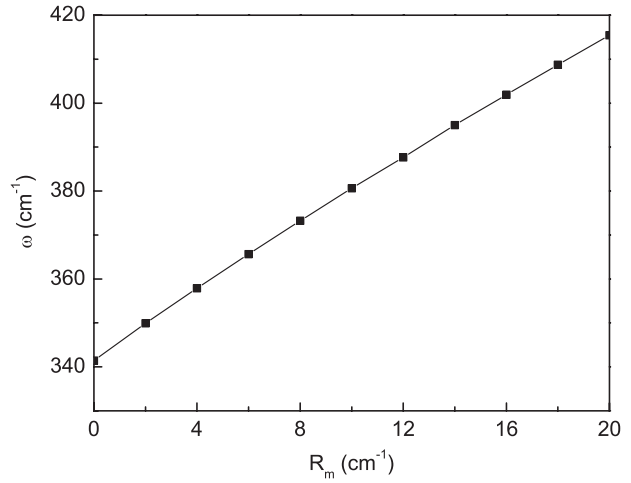

Figure 6. Dependence of the phonon energy ω on the bulk spin–phonon interaction constant $|R_m|$ for a multiferroic nanoparticle with $N = 7$ shells, $R_{ms}/R_m = 1.5$, $R_{es}/R_e = 1.5$ and $T = 300$ K.

spin–phonon interaction constant R_m is connected through the first and second derivatives with the exchange interaction constant $A_1(r_i - r_j)$ which depends on the distance between the neighbor spins. So it can be smaller when the distance is bigger, i.e. the radii of the ions are smaller, or greater for smaller distance, i.e. greater radius. So we have different R_m-values in different multiferroic compounds. With decreasing R_m, i.e. with decreasing radius of the rare earth ion, the anomaly around T_N is smaller, for example in $RMnO_3$ nanoparticles this could be the case for R = Y. The phonon energy shows a strong analogous dependence on the exchange interaction constant of the magnetic subsystem $A_1(r_i - r_j)$, which depends on the distance between the spins and indirectly on the radius of the ions. ω decreases with increasing A_1 (figure 7). The magnetic phase transition temperature T_N increases with increase of A_1.

In principle one can obtain different behaviors of the phonon frequencies, hardening or softening in the temperature

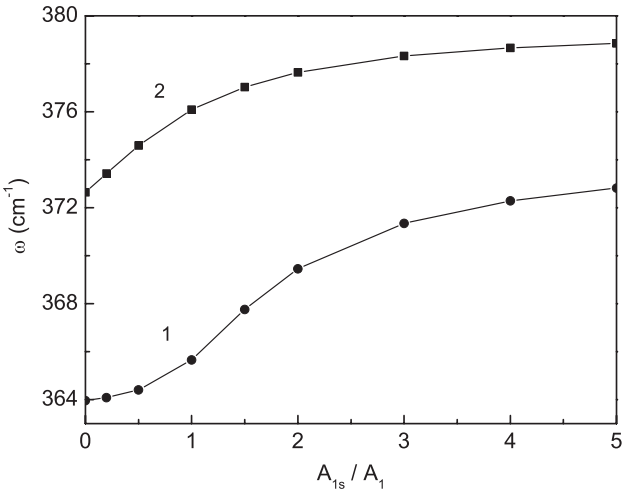

Figure 7. Dependence of the phonon energy ω on the surface magnetic interaction constant A_{1s}/A_1 for a multiferroic nanoparticle with $N = 7$ shells, $R_{ms}/R_m = 1.5$, $R_{es}/R_e = 1.5$ for different temperatures T: (1) 300; (2) 200 K.

regions below T_N and between T_N and T_C depending on the sign of R, softening for negative values and hardening for positive ones [2]. The different multiferroic substances have different interactions between the two subsystems and thus different R_m- and R_e-values, positive or negative. In $BiMnO_3$ and $YCrO_3$ there is an interaction between ferromagnetic and ferroelectric subsystems, in $YMnO_3$ and $BiFeO_3$—antiferromagnetic and ferroelectric [1]. In $BiCrO_3$ films recently it has been found that there is an interaction between antiferroelectricity and antiferromagnetism (or weak ferromagnetism) [30]. Modern studies of hexagonal $YMnO_3$ have revealed a coupling between the ferroelectric and magnetic ordering [31]. Evidence of the importance and the stronger influence of the spin–phonon interaction constant R_m is the increasing (or decreasing) of the phonon energy with increasing $|R_m|$ for $R_m < 0$ (or $R_m > 0$), independent of the sign of R_e.

We find that the phonon damping γ increases with temperature and with increasing R_m (for the two cases $R_m > 0$ and $R_m < 0$, because the damping is proportional to R_m^2) (figure 8). It is clearly seen that around the phase transition temperatures T_N and T_C there are strong anomalies in the phonon damping which is in agreement with the experimental data of Haumont *et al* [6]. The damping increases with increasing of the exchange interaction constants A_1 and J and with increasing of the anharmonic pseudo-spin–phonon interaction constants R_m and R_e.

The effect of the coupling constant between the magnetic and electric subsystems g on the phonon spectrum is shown in figures 9 and 10. It can be seen that the phonon energy ω depends strongly on g below T_N (figure 9). Above T_N it is independent of g. With raising of g the Néel temperature T_N increases and the kink around T_N disappears. The curves are not so steep at low temperatures. As already mentioned, ω depends also on the sign of the spin–phonon interaction R_m. With increasing g for T = const the phonon energy is enhanced for $R_m < 0$ and reduced for $R_m > 0$. There

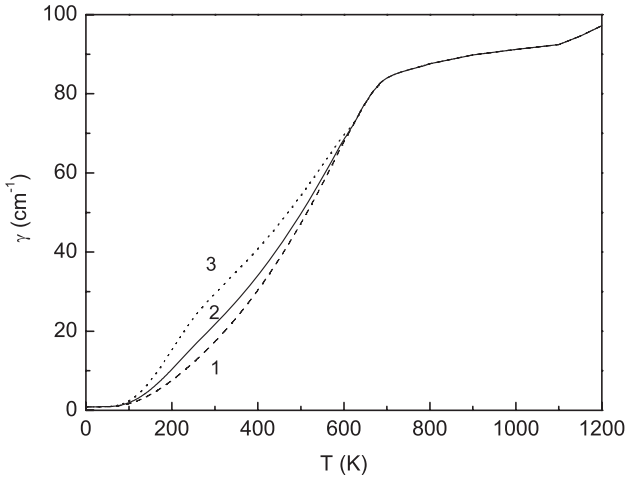

Figure 8. Temperature dependence of the phonon damping γ for a multiferroic nanoparticle with $N = 7$ shells, $R_{ms}/R_m = 1.5$, $R_{es}/R_e = 1.5$ and different bulk spin–phonon interaction constants $|R_m|$: (1) 2; (2) 6; (3) 10 cm^{-1}.

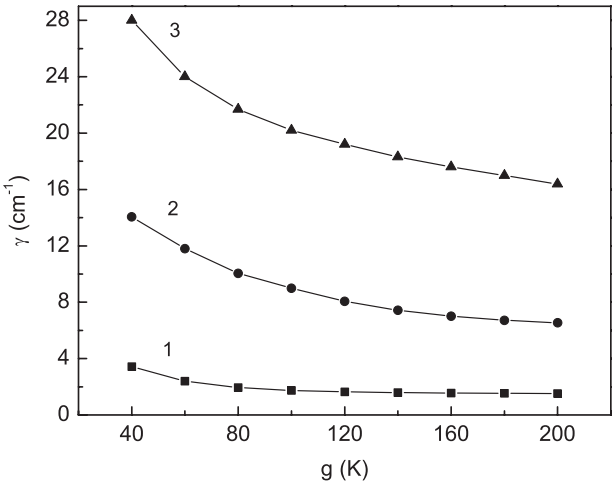

Figure 10. Dependence of the phonon damping γ on the magnetoelectric coupling constant g for a multiferroic nanoparticle with $N = 7$ shells, $R_{ms}/R_m = 1.5$, $R_{es}/R_e = 1.5$, and different temperatures T: (1) 100; (2) 300; (3) 300 K.

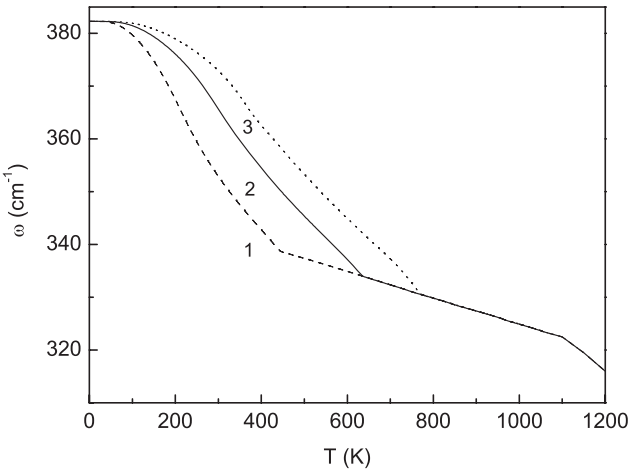

Figure 9. Temperature dependence of the phonon energy ω for a multiferroic nanoparticle with $N = 7$ shells, $R_{ms}/R_m = 1.5$, $R_{es}/R_e = 1.5$, and different magnetoelectric coupling constants g: (1) 40; (2) 80; (3) 120 K.

is experimental evidence of different coupling strengths and different coupling mechanisms between the magnetic and ferroelectric systems in different hexagonal multiferroics. The replacement of magnetic Ho for Y in $YMnO_3$ results in an even larger suppression of the thermal conductivity [32]. Sergienko *et al* [33] predicted that the polarization in $HoMnO_3$ is enhanced by up to two orders of magnitude with respect to that in $TbMnO_3$ where the ME interaction term is linear in the electrical dipole moment. The damping of the phonon mode γ decreases with increasing of the magnetoelectric constant g (figure 10). The decrease is stronger at higher temperatures. The damping can be observed from the full width at half maximum in Raman spectroscopic experiments. Sushkov *et al* [34] have obtained very different line widths in different multiferroic substances. The origin of the different widths is not quite clear. We have obtained that the damping of the phonon mode is strongly dependent on the magnetoelectric coupling g, on the exchange interaction constants A_1, J, and mostly on the spin–phonon interaction constants R_m and R_e. In figure 8 we show that the damping increases with increase of $|R_m|$. R_m is indirectly connected with the radius of the rare earth ion which is different in various multiferroics (see discussion after figures 5 and 6). So we have different R_m-values in various multiferroic compounds which leads to different damping values, i.e. to different line widths in different multiferroic substances. The different anharmonic spin–phonon interactions are one of the possible explanations of the different line widths in different multiferroic substances. The magnetoelectric coupling can also be different in the different multiferroic substances [32].

In order to study the size effects, we have calculated the dependence of the phonon energy and the phonon damping on the particle shell numbers N. The phonon energy ω can decrease or increase depending on the ratio R_{ms}/R_m and/or R_{es}/R_e with decreasing particle size, whereas the phonon damping increases always. With decreasing of N, ω decreases for the case where the surface constants are larger than the bulk ones $R_s/R_b < 1$ and increases for the other case $R_s/R_b > 1$. Kamba *et al* [10] and Singh *et al* [13] have observed that the Raman-mode frequencies in BFO ceramics and thin films are higher than the modes seen in single crystals [6]. In order to obtain this increase of the phonon energy in BFO nanostructures, we have to take parameters according to the second case $R_s/R_b > 1$ (figures 11 and 12). The phonon energy and the phonon damping increases with decreasing of particle size. This is in agreement with the experimental data of Popa *et al* [16]. They obtained reduced intensities and widened Raman peaks in BFO powders which could be related to the small crystal size of 7–11 nm within the powder particles.

The discussion above was done for $H = 0$. The influence of an applied magnetic field H on the phonon energy can be seen in figures 13 and 14. The phonon energy ω and the magnetic phase transition temperature T_N increase

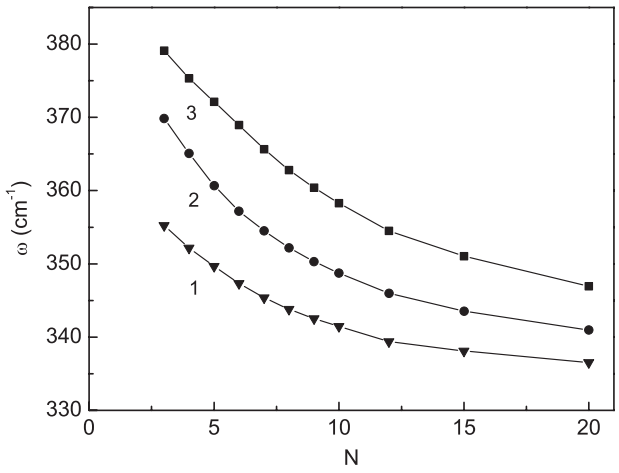

Figure 11. Dependence of the phonon energy ω on the particle size of a multiferroic nanoparticle with $R_{ms}/R_m = 1.5$, $R_{es}/R_e = 1.5$ for different temperatures T: (1) 500; (2) 400; (3) 300 K.

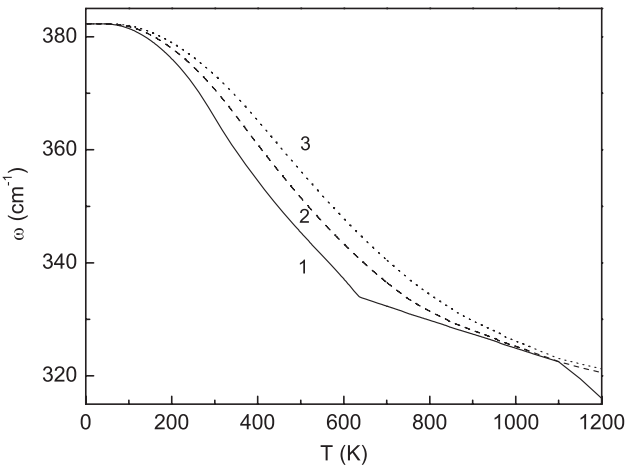

Figure 13. Temperature dependence of the phonon energy ω for $R_{ms}/R_m = 1.5$, $R_{es}/R_e = 1.5$, and different H-values: (1) $H = 0$, (2) 50; (3) 100 Oe.

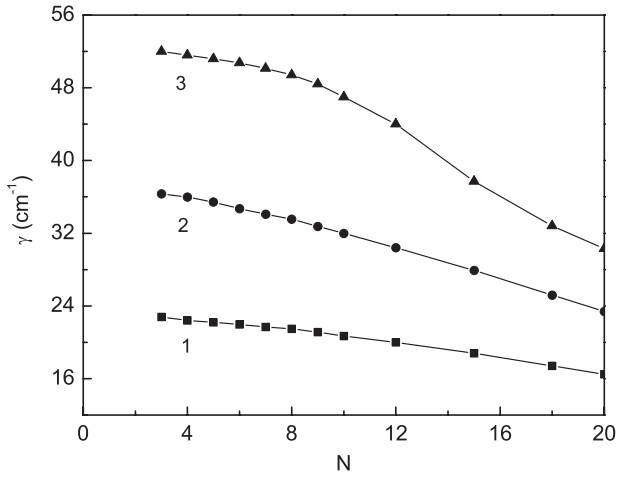

Figure 12. Dependence of the phonon damping γ on the particle size of a multiferroic nanoparticle with $R_{ms}/R_m = 1.5$, $R_{es}/R_e = 1.5$ for different temperatures T: (1) 300; (2) 400; (3) 500 K.

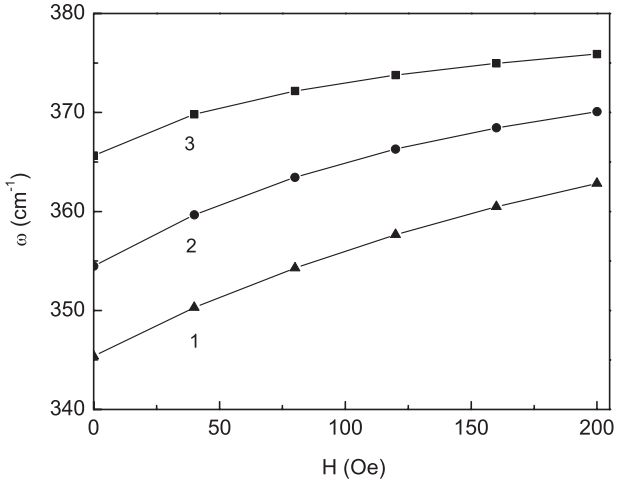

Figure 14. Magnetic field dependence of the phonon energy ω for $R_{ms}/R_m = 1.5$, $R_{es}/R_e = 1.5$, and different temperatures T: (1) 500; (2) 400; (3) 300 K.

with increasing H and the kink around T_N disappears. This is in qualitative agreement with the experimental data of Cheong [35]. The phonon damping decreases for larger values of the applied magnetic field H (figure 15) and the anomaly around T_N disappears, too. A similar increase of the phonon energy and decrease of the phonon damping with increasing magnetic field was observed in ferromagnetic nanoparticles by Yu *et al* [36].

5. Conclusions

The coexistence and interplay of different properties—magnetic, ferroelectric and phonon—in multiferroic nanoparticles has been investigated based on the Heisenberg and the transverse Ising models, taking into account the anharmonic spin–phonon and phonon–phonon interaction terms. We have obtained for the first time the temperature dependence of the phonon spectrum including damping effects for different magnetoelectric coupling, surface exchange interaction, and mostly for different surface spin–phonon interaction constants. The phonon energy and the phonon damping show strong anomalies around the magnetic and electric phase transition temperatures T_N and T_C, respectively, which are due to the magnetoelectric and to the spin–phonon interaction. With decreasing of the magnetic spin–phonon coupling R_m, i.e. decreasing of the radius of the rare earth ion in hexagonal $RMnO_3$ nanoparticles, the phonon frequency increases and the anomaly around T_N is smaller, for example for R = Y. We found that the phonon damping is strongly dependent on the magnetoelectric coupling g, on the exchange interaction constants A_1 and J, and on the spin–phonon interaction constants R_m and R_e. The different anharmonic spin–phonon interaction constants R_m (due, for example, to different rare earth ion radii or to different exchange interaction constants A_1) or/and the different magnetoelectric constants g are one of the possible explanations of the different line widths

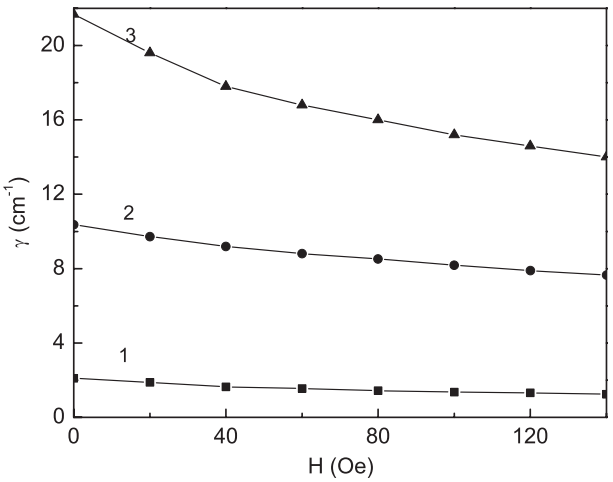

Figure 15. Magnetic field dependence of the phonon damping γ for $R_{ms}/R_m = 1.5$, $R_{es}/R_e = 1.5$, and different temperatures T: (1) 100: (2) 200; (3) 300 K.

obtained in different multiferroic substances. The phonon energy and the damping increase with decreasing particle size. The influence of an external magnetic field on the phonon spectrum of multiferroic nanoparticles was also calculated. We found that the phonon energy increases whereas the damping decreases with enhancing of H. The kink around T_N vanishes. The theoretical results are in qualitative agreement with the experimental data. Unfortunately not many experimental data exist for multiferroic nanoparticles.

Acknowledgment

This work was supported by the National Science Foundation of Bulgaria under Grand No. ID01/127.

References

[1] Fiebig M 2005 *J. Phys. D: Appl. Phys.* **38** R123
[2] Wesselinowa J M and Kovachev St 2007 *J. Phys.: Condens. Matter* **19** 386218
[3] Litvinchuk A P, Iliev M N, Popov V N and Gospodinov M M 2004 *J. Phys.: Condens. Matter* **16** 809
[4] Sharma A, Ahn J S, Hur N, Park S, Kim S B, Lee S, Park J-G, Guha S and Cheong S-W 2004 *Phys. Rev. Lett.* **93** 177202
[5] dela Cruz C, Yen F, Lorenz B, Wang Y Q, Sun Y Y, Gospodinov M M and Chu C W 2005 *Phys. Rev.* B **71** 060407(R)
[6] Haumont R, Kreisel J, Bouvier P and Hippert F 2006 *Phys. Rev.* B **73** 132101
[7] Fukumura H, Matsui S, Harima H, Takahashi T, Itoh T, Kisoda K, Tamada M, Noguchi Y and Miyayama M 2007 *J. Phys.: Condens. Matter* **19** 365224
[8] Singh M K, Katiyar R S and Scott J F 2008 *J. Phys.: Condens. Matter* **20** 252203
[9] Yuan G L, Or S W and Chan H L W 2007 *J. Appl. Phys.* **101** 064101
[10] Kamba S, Nuzhnyy D, Savonov M, Sebek J, Petzelt J, Prokleska J, Haumont R and Kreisel J 2007 *Phys. Rev.* B **75** 024403
[11] Seidel J, Kantner C L S, Chu Y-H, Yang L, Schlesinger Z, Viehland D, Orensten J and Ramesh R 2007 *APS March Mtg* N13.002
[12] Lobo R P S M, Moreira R L, Lebeugle D and Colson D 2007 *Phys. Rev.* B **76** 172105
[13] Singh M K, Jang H M, Ryu S and Jo M H 2006 *Appl. Phys. Lett.* **88** 042907
[14] Singh M K, Ryu S and Jang H M 2005 *Phys. Rev.* B **72** 132101
[15] Bea H, Bibes M, Petit S, Kreisel J and Barthelemy A 2007 *Phil. Mag. Lett.* **87** 165
[16] Popa M, Crespo D, Calderon-Moreno J M, Preda S and Fruth V 2007 *J. Am. Ceram. Soc.* **90** 2723
[17] Wesselinowa J M and Apostolova I 2008 *J. Appl. Phys.* **104** 084108
[18] Wesselinowa J M and Apostolova I 2008 *Solid State Commun.* **147** 94
[19] Blinc R and Zeks B *Soft Modes in Ferroelectrics and Antferroelectrics* (Amsterdam: North-Holland) p 1074
[20] Pirc R and Blinc R 2004 *Phys. Rev.* B **70** 134107
[21] Cao H X and Li Z Y 2003 *J. Phys.: Condens. Matter* **15** 6301
[22] Wesselinowa J M and Kovachev St 2007 *J. Appl. Phys.* **102** 043911
[23] Wesselinowa J M and Georgiev I 2008 *Phys. Status Solidi* b **245** 1653
[24] Tserkovnikov Yu A 1971 *Teor. Mat. Fiz.* **7** 250
[25] Wesselinowa J M and Apostolova I 2008 *Phys. Lett.* A **372** 305
[26] Ramirez M O, Krishnamurthi M, Denev S, Kumar A, Yang S-Y, Chu Y-H, Saiz E, Seidel J, Pyatakov A P, Bush A, Viehland D, Ornstein J, Ramesh R and Gopalan V 2008 *Appl. Phys. Lett.* **92** 022511
[27] Fukumura H, Matsui S, Tonari N, Nakamura T, Kisoda K, Hasuike N, Nishio K, Isshiki T and Harima H 2008 *E-MRS Fall Mtg, Symp. A*
[28] Fukumura H, Hasuike N, Harima H, Kisoda K, Fukae K, Takahashi T, Yoshimura T and Fujimura N 2007 *J. Phys.: Conf. Ser.* **92** 012126
[29] Hermet P, Goffinet M, Kreisel J and Ghosez P 2007 *Phys. Rev.* B **75** 220102(R)
[30] Lee N, Varela M and Christen H M 2006 *Appl. Phys. Lett.* **89** 162904
[31] Huang Z J, Cao Y, Sun Y Y, Xue Y Y and Chu C W 1997 *Phys. Rev.* B **56** 2623
[32] Sharma A, Ahn J S, Hur N, Park S, Kim S B, Lee S, Park J-G, Guha S and Cheong S-W 2004 *Phys. Rev. Lett.* **93** 177202
[33] Sergienko I A, Sen C and Dagotto E 2006 *Phys. Rev. Lett.* **97** 227204
[34] Sushkov A B, Aguliar R V, Park S, Cheong S-W and Drew H D 2007 *Phys. Rev. Lett.* **98** 027202
[35] Cheong S-W 2006 *Abstr. of Meeting (Tallini, Juli)* p 62
[36] Yu T, Shen Z X, Sun W X, Lin J Y and Ding J 2003 *J. Phys.: Condens. Matter* **15** L213